Primordial magnetic helicity evolution with a homogeneous magnetic field from inflation

Axel Brandenburg,[1, 2, 3, 4, 5] Ruth Durrer,[6] Yiwen Huang,[4, 7]

Tina Kahniashvili,[4, 5, 8, 9] Sayan Mandal *,[4, 5, †] and Shinji Mukohyama[10, 11]

[1]*Nordita, KTH Royal Institute of Technology and Stockholm University, Roslagstullsbacken 23, 10691 Stockholm, Sweden*
[2]*Department of Astronomy, AlbaNova University Center, Stockholm University, 10691 Stockholm, Sweden*
[3]*JILA and Laboratory for Atmospheric and Space Physics,*
University of Colorado, Boulder, Colorado 80303, USA
[4]*McWilliams Center for Cosmology and Department of Physics,*
Carnegie Mellon University, 5000 Forbes Avenue, Pittsburgh, Pennsylvania 15213, USA
[5]*Faculty of Natural Sciences and Medicine, Ilia State University, 3-5 Cholokashvili Street, 0194 Tbilisi, Georgia*
[6]*Département de Physique Théorique and Center for Astroparticle Physics,*
Université de Geneve, Quai Ernest Ansermet 24, 1211 Genéve 4, Switzerland
[7]*Department of Physics, University of California San Diego,*
9500 Gilman Drive 1110-115, La Jolla, California 92093
[8]*Abastumani Astrophysical Observatory, 47 Kostava Street, 0179 Tbilisi, Georgia*
[9]*Department of Physics, Laurentian University, Ramsey Lake Road, Sudbury, Ontario P3E 2C,Canada*
[10]*Center for Gravitational Physics, Yukawa Institute for Theoretical Physics, Kyoto University, Kyoto 606-8502, Japan*
[11]*Kavli Institute for the Physics and Mathematics of the Universe (WPI),*
The University of Tokyo Institutes for Advanced Study,
The University of Tokyo, Kashiwa, Chiba 277-8583, Japan

Motivated by a scenario of magnetogenesis in which a homogeneous magnetic field is generated during inflation, we study the magnetohydrodynamic evolution of the primordial plasma motions for two kinds of initial conditions – (i) a spatially homogeneous field with an unlimited correlation length, and (ii) a zero flux scale-invariant statistically homogeneous magnetic field. In both cases, we apply, for a short initial time interval, monochromatic forcing at a certain wave number so that the correlation length is finite, but much smaller than the typical length scale of turbulence. In particular, we investigate the decay of nonhelical and helical hydromagnetic turbulence. We show that, in the presence of a homogeneous magnetic field, the decay of helical and nonhelical small-scale fields can occur rapidly. This is a special property of a system with a perfectly homogeneous magnetic field, which is sometimes considered as a local approximation to a slowly varying background field. It can never change and acts as an imposed magnetic field. This is in a sharp contrast to the case of a statistically homogeneous magnetic field, where we recover familiar decay properties: a much slower decay of magnetic energy and a faster growth of the correlation length, especially in the case with magnetic helicity. The result suggests that a homogeneous magnetic field, if generated during inflation, should persist under the influence of small-scale fields and could be the origin of the large-scale magnetic field in the Universe.

PACS numbers:

I. INTRODUCTION

One of several open problems in cosmology and astrophysics is the understanding of the origin of large-scale magnetic fields in the Universe [1, 2]. There are two widely considered approaches to understand the origin of intercluster, large-scale correlated magnetic fields – (i) an *astrophysical* scenario [3], where weak seed fields generated by local sources are amplified and transferred to large scales by various astrophysical processes, and (ii) a *cosmological* (or primordial) scenario [4], where a strong seed magnetic field generated in the early universe evolves through magnetohydrodynamic (MHD) coupling with the primordial plasma. Neronov and Vovk [5] used the nonobservation of GeV photons from TeV blazars to put a lower limit on the strength of magnetic fields on extragalactic scales, obtaining a lower bound of $\sim 10^{-15}$ G at 1 Mpc. The limits were later revised to $\sim 10^{-18}$ G after considering that the observation period of the sources was limited to only a few years [6, 7]. The Fermi-LAT and the VERITAS collaborations have improved this limit again to $\sim 10^{-15}$ G at 1 Mpc [8, 9], based on ten years of observations of the TeV blazar emission spectra. These observational limits favor the cosmological (primordial) scenario of magnetogenesis [10]; see Ref. [11] for discussions on possible uncertainties in these lower limits based on blazar spectra and Refs. [12, 13] on possible impacts of plasma instabilities.

There are several scenarios for generating primordial magnetic fields in the early universe; see Ref. [14] for a review. Here we consider two main ideas. First, magnetic

fields can be generated during inflation or through processes related to it, like *reheating* or *preheating*. Reheating is the epoch at the end of inflation when the energy in the hypothesized inflaton field decays into the fields of the standard model and the temperature of the universe rises sufficiently. The decay of the inflaton into bosons can be very rapid owing to processes such as a parametric resonance or a tachyonic instability. Such a rapid decay is called preheating. Primordial magnetic fields can also be generated during cosmological phase transitions. The evolution of these primordial fields in the expanding universe has been studied by several authors by solving the MHD equations for the magnetic field, the density, and the velocity of the plasma; see Ref. [15] for a brief review and references within. The fields used are generally modeled either as *homogeneous*, or as *statistically homogeneous* and isotropic random Gaussian stochastic fields. Statistical homogeneity implies that the two-point correlation function of the magnetic field is independent of the position in space. In this paper, we show that these two approaches can result in very different dynamics of the induced turbulent motions in the early universe. In particular for the former case, small-scale helical and nonhelical fields decay in a way very different from the case of statistically homogeneous fields, as discussed below.

While there were earlier ideas suggesting the presence of a homogeneous magnetic field [16–18], those papers study just cosmological consequences without specifying or discussing a generation mechanism. While Ref. [19] discusses the generation of a homogeneous magnetic field, it assumes the existence of "protogalaxies" with angular momentum in the radiation dominated epoch, which contradicts with the current understanding of our Universe. Reference [20] also discusses a generation mechanism but it assumes a tachyonic mass for a gauge field, which means that the corresponding Higgs field is a ghost and thus the model is unstable. While the model in Ref. [21] is similar to gauge-flation or chromo-natural inflation, what is called a magnetic field there is simply due to the nonlinear part of the field strength and is thus actually an electric field, if a part of the non-Abelian gauge field is projected onto an Abelian gauge field via a spontaneous symmetry breaking (e.g., $SU(2) \times U(1) \to U(1)$) or if their ansatz of the gauge potential is applied to an Abelian gauge field. As far as the authors know, no stable generation mechanism of homogeneous magnetic fields has been proposed until recently. (In open Universes, while one might hope to find such a mechanism through supercurvature modes, but it is known that there is actually no supercurvature mode for vector fields [14].) However, the lack of a generation mechanism does not necessarily mean a lack of interest in homogeneous magnetic fields. Indeed, as already mentioned above, the studies of cosmological consequences of a homogeneous magnetic field date back to the seminal works by Zel'dovich, Doroshkevich, and Thorne in 1960'=s.

Recently, one of the authors [22] proposed a stable generation mechanism of homogeneous magnetic field, based on a $U(1)$ gauge theory of electromagnetism with a coupling to Horndeski type *scalar-tensor gravity*, where gravity is described by the metric tensor field and an additional scalar field[1]. During inflation, the model admits a stable (quasi) de Sitter solution with a homogeneous magnetic field as an attractor of the system. Therefore the model provides a classical generation mechanism of homogeneous magnetic fields during inflation. After inflation and the stabilization of the scalar field at the minimum of its potential, on the other hand, gravity is effectively described by general relativity. Later in the present paper, we show that the action after inflation is the Einstein-Maxwell action, supplemented with a nonminimal coupling between curvature and electromagnetism. We also show that, upon imposing observational constraints, the nonminimal coupling can be ignored for the analysis of the magnetic field evolution. This in particular means that the no-minimal coupling does not introduce new instabilities in the homogeneous magnetic field background in the late-time cosmology.

It was already known that in the additional presence of primordial small-scale turbulence, the magnetic energy spectrum changes only very little at large length scales [25]. This led one of the authors [22] to expect that this also applies to the case of a homogeneous magnetic field, but this remained to be verified by numerical MHD simulations. It is therefore important to study the MHD evolution of primordial plasma motions in the presence of these homogeneous magnetic fields, which is what we focus on in this work.

We are particularly interested in the evolution of magnetic helicity, which is known not to be conserved in a periodic domain in the presence of a homogeneous magnetic field [26]. However, if we were to consider a perfectly homogeneous magnetic field as a local approximation to a slowly varying background magnetic field, magnetic helicity conservation would be restored. To illuminate the remarkable properties of a perfectly homogeneous magnetic field, we also discuss the alternative approach of working instead with a statistically homogeneous magnetic field, which does not impose any constraints on the magnetic helicity evolution. The presence of magnetic helicity substantially changes the decay rate for MHD turbulence [27]. In this paper we compare the decay dynamics for homogeneous and statistically homogeneous magnetic fields with a scale-invariant spectrum. In previous works, we have studied only statistically homogeneous magnetic fields induced by the turbulence dynamics [28] but did not include the turbulence in the presence of a homogeneous magnetic field.

This paper is arranged as follows. The model is described in Sec. II, where we discuss the formalism for how a spatially homogeneous magnetic field is realized during inflation, and after that until recombination. In

---

[1] See, e.g., [23] for more details about scalar-tensor gravity.

Sec. III, we describe in detail the setup of our simulations, discussing, in particular, various initial conditions to examine peculiar features associated with the use of an imposed magnetic field. We present numerical solutions in Sec. IV and in Sec. V, we present our conclusions. Throughout this paper we work in natural units where $\hbar = c = 1$, and our metric signature is $(-, +, +, +)$. For the electromagnetic quantities we use Lorentz-Heaviside units.

II. HOMOGENEOUS MAGNETIC FIELDS

In this section we briefly describe a theoretical framework in which a spatially homogeneous magnetic field background can be realized during and after inflation in the early Universe. In the inflationary stage, the background spacetime is not only homogeneous but also isotropic despite the existence of the preferred spatial direction defined by the homogeneous magnetic field. This is made possible by a nonlinear kinetic action for the $U(1)$ gauge field nonminimally coupled to a scalar-tensor theory of gravity. In the postinflationary stage, on the other hand, the scalar field is stabilized around a minimum of a potential and thus the theory is reduced to the Einstein-Maxwell theory supplemented with the Horndeski's nonminimal coupling. Therefore, after inflation the spacetime becomes anisotropic and the homogeneous magnetic field adiabatically decays. If we are interested in the postinflationary evolution of the $U(1)$ gauge field at subhorizon scales for timescales sufficiently shorter than the cosmological time then the gravitational effects of and on the gauge field can be neglected and the system is described by the standard Maxwell theory expanded around the homogeneous magnetic field background in Minkowski spacetime. As we shall see in the next sections, the existence of the homogeneous magnetic field significantly affects the evolution of the gauge field at subhorizon scales.

A. General action

We consider a metric $g_{\mu\nu}$, a $U(1)$ gauge field A_μ and a scalar field ϕ in four dimensional spacetime described by the action

$$I = \int d^4x \sqrt{-g} \left[L + L_3 + L_4 + L_5 + L_{\mathrm{H}} \right], \quad (1)$$

where $L = L(\phi, X, W, Y, Z)$ is an arbitrary function of ϕ,

$$X \equiv -\frac{1}{2} g^{\mu\nu} \partial_\mu \phi \partial_\nu \phi, \quad W \equiv -\frac{1}{4} \mathcal{F}_{\mu\nu} \mathcal{F}^{\mu\nu},$$

$$Y \equiv \mathcal{F}_{\mu\nu} \tilde{\mathcal{F}}^{\mu\nu}, \quad Z \equiv \mathcal{F}^{\rho\mu} \mathcal{F}_\rho{}^\nu \partial_\mu \phi \partial_\nu \phi; \quad (2)$$

$\mathcal{F}_{\mu\nu}$ and $\tilde{\mathcal{F}}^{\mu\nu}$ are defined by

$$\mathcal{F}_{\mu\nu} \equiv e^\phi F_{\mu\nu}, \quad \tilde{\mathcal{F}}^{\mu\nu} \equiv e^\phi \tilde{F}^{\mu\nu},$$

$$F_{\mu\nu} \equiv \partial_\mu A_\nu - \partial_\nu A_\mu, \quad \tilde{F}^{\mu\nu} \equiv \frac{1}{2} \epsilon^{\mu\nu\rho\sigma} F_{\rho\sigma}, \quad (3)$$

and $\epsilon^{0123} = -1/\sqrt{-g}$;

$$L_3 = -G_3(\phi, X) \Box \phi,$$
$$L_4 = G_4(\phi, X) R + G_{4X}(\phi, X) \left[(\Box\phi)^2 - (\nabla^\mu \nabla_\nu \phi)(\nabla^\nu \nabla_\mu \phi) \right],$$
$$L_5 = G_5(\phi, X) G^{\mu\nu} \nabla_\mu \nabla_\nu \phi - \frac{1}{6} G_{5X}(\phi, X) \left[(\Box\phi)^3 \right.$$
$$- 3(\Box\phi)(\nabla^\mu \nabla_\nu \phi)(\nabla^\nu \nabla_\mu \phi)$$
$$\left. + 2(\nabla^\mu \nabla_\nu \phi)(\nabla^\nu \nabla_\rho \phi)(\nabla^\rho \nabla_\mu \phi) \right] \quad (4)$$

are Horndeski scalar terms [29, 30]; and

$$L_{\mathrm{H}} = \xi(\phi) \tilde{\mathcal{F}}^{\mu\nu} \tilde{\mathcal{F}}^{\rho\sigma} R_{\mu\nu\rho\sigma} \quad (5)$$

is a simple modification of Horndeski's nonminimal coupling of the $U(1)$ gauge field to the Riemann tensor $R^\mu{}_{\nu\rho\sigma}$ of the metric $g_{\mu\nu}$ [31]. Here, the scalar field ϕ and the gauge field A_μ are normalized so that their mass dimensions are zero, $G_{3,4,5}(\phi, X)$ are arbitrary functions of ϕ and X, the subscript X denotes derivative with respect to X, and $\xi(\phi)$ is an arbitrary function of ϕ. The action is invariant under the $U(1)$ gauge transformation,

$$A_\mu \to A_\mu + \partial_\mu \lambda, \quad (6)$$

where λ is an arbitrary function, and the equations of motion are second-order differential equations. In principle it is possible to consider a more general form of L that depends on the second covariant derivatives of ϕ and A_μ without introducing higher derivatives in the equations of motion. For simplicity, however, we restrict our consideration to the above form of L that depends on only up to first derivatives of ϕ and A_μ. Also, the inclusion of the factor e^ϕ in the definitions of $\mathcal{F}_{\mu\nu}$ and $\tilde{\mathcal{F}}^{\mu\nu}$ is redundant since we allow for the explicit ϕ-dependence of $L(\phi, X, W, Y, Z)$ and $\xi(\phi)$. We nonetheless adopt the above definitions of $\mathcal{F}_{\mu\nu}$ and $\tilde{\mathcal{F}}^{\mu\nu}$ including the factor e^ϕ in order to make it easy to implement a scaling-type symmetry for the description of the system during the inflationary stage [see Eqs. (7) and (8) in the next subsection).

B. Stealth magnetic field during inflation

Following the discussion in Sec. V of [22], we suppose that the main source of curvature perturbations is not ϕ but something else. For example, one can introduce another scalar field as an inflaton or a curvaton. For simplicity we approximate the geometry during inflation by a de Sitter spacetime. Then the effective cosmological constant induced by the field responsible for curvature perturbations simply amounts to a constant shift of $L(\phi, X, W, Y, Z)$.

In order to simplify the analysis and also to allow for an exact solution that represents a de Sitter spacetime with a homogeneous magnetic field, we require that the action is invariant under not only the $U(1)$ gauge transformation (6) but also the following scaling-type global transformation for the range of ϕ that is relevant for the inflationary epoch.

$$\phi \to \phi + \phi_0\,, \quad A_\mu \to e^{-\phi_0}A_\mu\,, \qquad (7)$$

where ϕ_0 is an arbitrary constant that is not too large to eject ϕ from the inflationary range. Then for the range of ϕ, the explicit ϕ-dependence of the functions $L(\phi, X, W, Y, Z)$, $G_{3,4,5}(\phi, X)$ and $\xi(\phi)$ is forbidden so that

$$
\begin{aligned}
L(\phi, X, W, Y, Z) &= \bar{L}(X, W, Y, Z)\,, \\
G_{3,4,5}(\phi, X) &= \bar{G}_{3,4,5}(X)\,, \\
\xi(\phi) &= \bar{\xi}\,,
\end{aligned}
\qquad (8)
$$

where $\bar{L}(X, W, Y, Z)$ is an arbitrary function of $(X,\,W,\,Y,\,Z)$, $\bar{G}_{3,4,5}(X)$ are arbitrary functions of X and $\bar{\xi}$ here is a constant. We also impose the parity invariance so that the function $\bar{L}(X, W, Y, Z)$ is even with respect to Y.

$$\bar{L}(X, W, Y, Z) = \bar{L}(X, W, -Y, Z)\,. \qquad (9)$$

This is the system studied in [22, 32].

For this system, we adopt the ansatz of the form

$$
\begin{aligned}
g_{\mu\nu}dx^\mu dx^\nu = &-N(t)^2 dt^2 \\
&+ a(t)^2\left[e^{4\sigma(t)}dx^2 + e^{-2\sigma(t)}(dy^2 + dz^2)\right]\,, \\
\phi = &\ \phi(t)\,, \\
A_t = 0\,, \quad &A_x = \int^t \frac{N(t')e^{4\sigma(t')}}{a(t')}E(t')dt'\,, \\
A_y = \frac{1}{2}Bz\,, \quad &A_z = -\frac{1}{2}By\,,
\end{aligned}
\qquad (10)
$$

where B is a constant. It was found in [22] that the equations of motion admit solutions of the form

$$
\begin{aligned}
H = \text{const.} > 0\,, \quad \Sigma = \text{const.}\,, \quad \chi = \text{const.} > 0\,, \\
E = \text{const.}\,, \quad B \neq 0\,,
\end{aligned}
\qquad (11)
$$

where

$$H \equiv \frac{\dot{a}}{Na}\,, \quad \Sigma \equiv \frac{\dot{\sigma}}{N}\,, \quad \chi \equiv \frac{e^\phi e^{2\sigma}}{a^2}\,. \qquad (12)$$

By tuning one parameter in the action, the solution is reduced to a de Sitter spacetime with magnetic field but without electric field [22], i.e.

$$
\begin{aligned}
H = \text{const.} > 0\,, \quad \Sigma = 0\,, \quad \chi = \text{const.} > 0\,, \\
E = 0\,, \quad B \neq 0\,.
\end{aligned}
\qquad (13)
$$

The reason why fine-tuning of just one parameter leads to two equalities, $\Sigma = 0$ and $E = 0$, is that we have imposed

the discrete symmetry (9). Reference [22] also found the condition under which the de Sitter solution with magnetic field but without electric field is an attractor of the system within the ansatz (10). Reference [32] then analyzed general linear perturbations around the attractor solution and found the condition under which the system of linear perturbations is free from instabilities.

In the present paper we consider the stable attractor de Sitter solution with magnetic field but without electric field as the origin of magnetic fields that are observed in the late-time Universe. We denote the (approximately) constant value of H during inflation as H_{inf} [2].

C. Postinflationary system

Following again the discussion in Sec. V of [22], we suppose that the scaling-type global symmetry (7) is not respected for the range of ϕ that is relevant for the postinflationary epoch so that the scalar field ϕ is stabilized at a local minimum of a potential, which we denote as ϕ_f. The action of the system is still supposed to be of the general form considered in Sec. II A. Assuming that the mass of ϕ around the local minimum of the potential is large enough, we integrate out ϕ by setting $\phi = \phi_f$ (and thus $X = 0$ and $\nabla_\mu\nabla_\nu\phi = 0$) in the general action. We then end up with the following action for the system after inflation.

$$
\begin{aligned}
I = \int d^4x\sqrt{-g}\,[&G_4(\phi_f, 0)R + L(\phi_f, 0, W_f, Y_f, 0) \\
&+ \xi(\phi_f)e^{2\phi_f}F_{\mu\nu}F_{\rho\sigma}R^{\mu\nu\rho\sigma}]\,,
\end{aligned}
\qquad (14)
$$

where

$$W_f \equiv -\frac{1}{4}e^{2\phi_f}F_{\mu\nu}F^{\mu\nu}\,, \quad Y_f \equiv e^{2\phi_f}F_{\mu\nu}\tilde{F}^{\mu\nu}\,. \qquad (15)$$

By Taylor expanding $L(0, W_f, Y_f, 0)$ with respect to W_f and Y_f up to first order and using the discrete symmetry (9), we obtain the low-energy effective action

$$
\begin{aligned}
I = \int d^4x\sqrt{-g}\bigg[&\frac{M_{\text{Pl}}^2}{2}(R - 2\Lambda) - \frac{1}{4}F^{(\text{post})}_{\mu\nu}F^{(\text{post})\mu\nu} \\
&+ \frac{\lambda}{4M_{\text{Pl}}^2}\tilde{F}^{(\text{post})}_{\mu\nu}\tilde{F}^{(\text{post})}_{\rho\sigma}R^{\mu\nu\rho\sigma}\bigg]\,,
\end{aligned}
\qquad (16)
$$

where we have assumed that

$$G_4(\phi_f, 0) > 0\,, \quad L_W(\phi_f, 0, 0, 0, 0) > 0\,, \qquad (17)$$

and introduced

$$M_{\text{Pl}} \equiv \sqrt{2G_4(\phi_f, 0)}\,, \quad \Lambda \equiv -\frac{L(\phi_f, 0, 0, 0, 0)}{M_{\text{Pl}}^2}\,, \qquad (18)$$

---

[2] In Refs. [22, 32] it was denoted as H_0.

$$\lambda \equiv \frac{4M_{\text{Pl}}^2 \xi(\phi_f)}{L_W(\phi_f, 0, 0, 0, 0)} \,, \quad F_{\mu\nu}^{(\text{post})} = e^{\phi_f} \sqrt{L_W(\phi_f, 0, 0, 0, 0)} F_{\mu\nu} \,,$$

and

$$\tilde{F}_{\mu\nu}^{(\text{post})} \equiv \frac{1}{2} \epsilon_{\mu\nu}{}^{\rho\sigma} F_{\rho\sigma}^{(\text{post})} \,. \tag{19}$$

Here, the subscript W denotes partial derivative with respect to W. So far, we have not yet fixed the overall normalization of $F_{\mu\nu}$ except that the mass dimension of A_μ is zero. We now fix the normalization as

$$e^{2\phi_f} L_W(\phi_f, 0, 0, 0, 0) = M_{\text{Pl}}^2 \,, \tag{20}$$

so that

$$\lambda \equiv 4e^{2\phi_f} \xi(\phi_f) \,, \quad F_{\mu\nu}^{(\text{post})} = M_{\text{Pl}} F_{\mu\nu} \,. \tag{21}$$

The postinflationary system described by the action (16) is nothing but the Einstein-Maxwell system supplemented with the Horndeski's nonminimal coupling.

Hereafter, we omit the superscript "(post)" so that the action for the postinflationary system is

$$\begin{aligned} I = \int d^4x \sqrt{-g} \Big[&\frac{M_{\text{Pl}}^2}{2}(R - 2\Lambda) - \frac{1}{4} F_{\mu\nu} F^{\mu\nu} \\ &+ \frac{\lambda}{4M_{\text{Pl}}^2} \tilde{F}_{\mu\nu} \tilde{F}_{\rho\sigma} R^{\mu\nu\rho\sigma} \Big] \,. \end{aligned} \tag{22}$$

D. Observational bounds on λ, H_{inf}, and σ

In Ref. [22], assuming that the stabilization of ϕ to the constant value ϕ_f occurs immediately after inflation and that the reheating process is instantaneous, the present amplitude of the large-scale magnetic field was estimated as

$$\mathcal{B}_{\text{today}} \simeq e^{-\phi_f} |b| \times 10^{-6}\,\text{G} \,, \tag{23}$$

where $b \equiv B/H_{\text{inf}}$. Also, [32] found several examples of parameters for which the system of linear perturbations is free from instabilities. In those examples, both b and g_h are nonvanishing and of order unity, where

$$g_h \equiv \xi \frac{H_{\text{inf}}^2}{M_{\text{Pl}}^2} \,, \tag{24}$$

and ξ is the constant value of $\xi(\phi)$ for the range of ϕ relevant for the inflationary epoch as already stated around (8). Under the assumption of immediate stabilization of ϕ after inflation, we have $\xi(\phi_f) = \xi$. Combining all these and the definition of λ given in (21), one obtains

$$\lambda \simeq 4 \times \left(\frac{\mathcal{B}_{\text{today}}}{|b| \times 10^{-6}\,\text{G}} \right)^{-2} \left(\frac{H_{\text{inf}}}{M_{\text{Pl}}} \right)^{-2} g_h \,. \tag{25}$$

The upper bound on the large scale magnetic field is roughly $10^{-9}\,\text{G}$ [33] and the lower bound from the blazar observations is roughly

$$10^{-15}\,\text{G} \lesssim \mathcal{B}_{\text{today}} \lesssim 10^{-9}\,\text{G} \,. \tag{26}$$

On the other hand, constraints on λ can be obtained by demanding that the nonminimal coupling term is less important than the standard Maxwell term [41]. Reference [42] applied this idea to neutron stars and found a conservative bound on λ as

$$|\lambda| \ll 10^{70} \,. \tag{27}$$

Combining (27) with (25), one obtains a lower bound on the inflation scale,

$$H_{\text{inf}} \gg |b| \, |g_h|^{1/2} \left(\frac{\mathcal{B}_{\text{today}}}{10^{-9}\,\text{G}} \right)^{-1} \times 10^{-15}\,\text{GeV} \,. \tag{28}$$

For the range (26) of $\mathcal{B}_{\text{today}}$ and $\mathcal{O}(1)$ values of b and g_h, this is not a strong constraint. Under the assumption of instantaneous reheating ($T_{\text{reh}} \sim \sqrt{M_{\text{Pl}} H_{\text{inf}}}$), Eq. (28) can be rewritten as a lower bound on the reheating temperature.

$$T_{\text{reh}} \gg |b|^{1/2} \, |g_h|^{1/4} \left(\frac{\mathcal{B}_{\text{today}}}{10^{-9}\,\text{G}} \right)^{-1/2} \times 100\,\text{GeV} \,. \tag{29}$$

One can also obtain limits on the parameter σ which characterizes the degree of axisymmetry of the Bianchi-I spacetime from its contribution to the quadrupole component C_2 of the power spectrum of temperature anisotropies of the cosmic microwave background (CMB). This contribution can be written as $C_2 = 16\pi(\sigma_{\text{dec}} - \sigma_0)^2/25$ (see Ref. [34] for an outline of the calculation), where σ_{dec} and σ_0 are values of σ at the decoupling and at the present, respectively. From the observed CMB quadrupole of $C_2^{\text{obs}} = 230\,\mu\text{K}^2/T_0^2$, where T_0 is the CMB temperature today. We can always normalize our coordinates such that $\sigma_0 = \sigma(t_0) = 0$ so that C_2 provides an upper bound on $|\sigma_{\text{dec}}|$,

$$|\sigma_{\text{dec}}| \lesssim 4 \times 10^{-6} \,. \tag{30}$$

E. Subhorizon description of postinflationary system

In general the effects of the nonminimal coupling can be ignored if

$$\frac{(\text{curvature})}{M_{\text{Pl}}^2} \ll \frac{1}{|\lambda|} \,. \tag{31}$$

For the Friedmann-Lemaître-Robertson-Walker (FLRW) cosmology, we have (curvature) $\sim T^4/M_{\text{Pl}}^2$, where T is the temperature of the Universe, and thus the nonminimal coupling can be ignored if

$$T \ll \left| \frac{\lambda}{10^{70}} \right|^{-1/4} \times 10\,\text{GeV} \,. \tag{32}$$

Therefore, imposing the conservative bound (27), we conclude that the evolution of the FLRW background cosmology during and after nucleosynthesis can be described

by the standard Einstein-Maxwell theory without the nonminimal coupling. For a local magnetic field with the amplitude $\mathcal{B}_{\text{local}}$, the induced curvature is of order (curvature) $\sim \mathcal{B}_{\text{local}}^2/(8\pi M_{\text{Pl}}^2)$ and thus the nonminimal coupling can be ignored if

$$\mathcal{B}_{\text{local}} \ll \left| \frac{\lambda}{10^{70}} \right|^{-1/2} \times 10^{21}\,\text{G}\,. \qquad (33)$$

Assuming that the conservative bound (27) is satisfied, the right-hand side is larger than $10^{21}\,\text{G}$ and thus the maximum amplitude of the magnetic field in the simulations studied in the next sections satisfies this condition. Therefore, we can safely ignore the effects of the nonminimal coupling and the theory is reduced to the standard Einstein-Maxwell theory without the nonminimal coupling.

For the standard Einstein-Maxwell theory in a radiation dominated Universe without the nonminimal coupling, the propagation speed of all physical degrees of freedom is of order unity and the Jeans scale is of order the Hubble scale. If we are interested in phenomena whose length and timescales are sufficiently shorter than the Jeans scales and the cosmological scales then the evolution of the system can be well described without taking into account the metric perturbation and the background cosmological expansion. On these scales, the system is well described by the standard Maxwell theory expanded around the homogeneous magnetic field background in Minkowski spacetime.

III. MAGNETIC FIELD EVOLUTION

In the previous section, we have discussed how a spatially homogeneous magnetic field can be realized during inflation, and more importantly, after the end of inflation. We now turn our attention to the study of the MHD evolution of such fields.

A. Basic equations

We study the time evolution in the presence of a homogeneous magnetic field right after inflation. In particular, we study the evolution of an additional field with some typical wave number k_*, which we induce by a random forcing term present during a short initial time interval. In the radiation dominated era, the primordial plasma is a relativistic, isothermal gas with energy density ρ and equation of state $w = 1/3$. In Lorentz-Heaviside units,

the MHD equations for such a gas are [43–45]

$$\frac{\partial \ln \rho}{\partial t} = -\frac{4}{3}\left(\nabla \cdot \mathbf{u} + \mathbf{u} \cdot \nabla \ln \rho\right)$$
$$+\frac{1}{\rho}\left[\mathbf{u} \cdot (\mathbf{J} \times \mathbf{B}) + \eta \mathbf{J}^2\right], \qquad (34)$$

$$\frac{\partial \mathbf{u}}{\partial t} = -(\mathbf{u} \cdot \nabla)\mathbf{u} + \frac{\mathbf{u}}{3}\left(\nabla \cdot \mathbf{u} + \mathbf{u} \cdot \nabla \ln \rho\right)$$
$$-\frac{1}{4}\nabla \ln \rho + \frac{3}{4\rho}\mathbf{J} \times \mathbf{B} + \frac{2}{\rho}\nabla \cdot (\rho \nu \mathsf{S})$$
$$-\frac{\mathbf{u}}{\rho}\left[\mathbf{u} \cdot (\mathbf{J} \times \mathbf{B}) + \eta \mathbf{J}^2\right] + \boldsymbol{\mathcal{F}}_0, \qquad (35)$$

$$\frac{\partial \mathbf{B}}{\partial t} = \nabla \times (\mathbf{u} \times \mathbf{B} - \eta \mathbf{J}) + \boldsymbol{\mathcal{E}}_0, \qquad (36)$$

where $\mathsf{S}_{ij} = \frac{1}{2}(u_{i,j} + u_{j,i}) - \frac{1}{3}\delta_{ij}\nabla \cdot \mathbf{u}$ are the components of the traceless rate-of-strain tensor, ν is the kinematic viscosity, η is the magnetic diffusivity, $\boldsymbol{\mathcal{F}}_0 = \mathcal{F}_0 \boldsymbol{f}$ and $\boldsymbol{\mathcal{E}}_0 = \mathcal{E}_0 \boldsymbol{f}$ are forcing terms, and

$$\boldsymbol{f}(\boldsymbol{x}, t) = \text{Re}\{\mathcal{N}\tilde{\boldsymbol{f}}(\boldsymbol{k}, t)\exp[i\boldsymbol{k} \cdot \boldsymbol{x} + i\phi]\}, \qquad (37)$$

is a forcing function that consists of random, white-in-time, plane waves with a certain average wave number k_* [46]. Here, $\boldsymbol{x}$ is the position vector and $\mathcal{N} = \sqrt{c_{\text{s}}^3 k_*}$ is a normalization factor with $c_{\text{s}} = \sqrt{w} = 1/\sqrt{3}$ being the speed of sound; see Ref. [46] for details. At each time step, we select randomly the phase $-\pi < \phi \le \pi$, the direction of a unit vector $\hat{\boldsymbol{e}}$, and the components of the wave vector $\boldsymbol{k}$ from many possible discrete wave vectors in a certain range around a given value of k_*. The Fourier amplitudes are

$$\tilde{\boldsymbol{f}}(\boldsymbol{k}) = \mathsf{R} \cdot \tilde{\boldsymbol{f}}(\boldsymbol{k})^{\text{(nohel)}} \quad \text{with} \quad \mathsf{R}_{ij} = \frac{\delta_{ij} - i\sigma\epsilon_{ijk}\hat{k}}{\sqrt{1 + \sigma^2}}, \quad (38)$$

where the parameter σ characterizes the fractional helicity of $\boldsymbol{f}$, and

$$\tilde{\boldsymbol{f}}(\boldsymbol{k})^{\text{(nohel)}} = (\boldsymbol{k} \times \hat{\boldsymbol{e}})\,/\,\sqrt{\boldsymbol{k}^2 - (\boldsymbol{k} \cdot \hat{\boldsymbol{e}})^2} \qquad (39)$$

is a nonhelical forcing function. We use only those $\hat{\boldsymbol{e}}$ that are not aligned with $\boldsymbol{k}$. Note that $|\tilde{\boldsymbol{f}}|^2 = 1$. We consider both $\sigma = 0$ and $\sigma = 1$, corresponding to the nonhelical and maximally helical cases. The forcing is only enabled during the time interval $0 \le t \le t_*$. In this sense, this forcing procedure can be considered as part of the initial condition.

In this section and henceforth, we use t to refer to conformal time, as opposed to coordinate time in Sec. II. All other quantities are comoving quantities, scaled by exploiting the conformal symmetry of Maxwell's equations; see [43] for details. We solve Eqs. (34)–(36) using the PENCIL CODE, a public MHD code[3], which is

---

[3] https://github.com/pencil-code

well suited for studying and simulating turbulence. The simulations are performed in a periodic domain of size L. Except for the homogeneous imposed magnetic field at wave number $k = 0$, the smallest nonvanishing wave number in the domain is $k_1 \equiv 2\pi/L$. Spatial derivatives are computed using sixth order accurate finite differences and a third order accurate time stepping scheme is used. The magnetic vector potential is advanced in time to preserve solenoidality (the divergence-free condition) of the magnetic field. We use a numerical resolution of 1152^3 meshpoints for all simulations presented in this paper.

B. Peculiarities connected with imposed fields

In a periodic domain, the case of an imposed magnetic field is in many ways pathological, since it will always be present and can never decay. It can be amplified linearly in time by a flow – even in two dimensions where no dynamo effect is possible [47]. In addition, magnetic helicity associated with the induced magnetic field based on the deviations of the magnetic field from the imposed field is not conserved [26]. This is because it interacts with the imposed field, which, owing to its constancy in space, cannot have magnetic helicity. On the other hand, if we replace the imposed field by a large-scale field with zero net flux, the magnetic helicity becomes well defined. The total field can then decay to zero, and the magnetic helicity is now a perfectly defined quantity that obeys the usual conservation law. We can therefore ask how the presence of a large-scale magnetic field affects the evolution of magnetic helicity of a field of much smaller length scale.

To better understand the aforementioned peculiarities, we note that in the presence of an imposed magnetic field, a generalized quantity can be defined that is still conserved [48], but that quantity is not gauge invariant and hence not uniquely defined [49]. Let us discuss this here in more detail. In the presence of an imposed field, $\mathbf{B}_0 = \text{const}$, one splits the magnetic field into a mean and a fluctuating component, $\mathbf{B} = \mathbf{B}_0 + \mathbf{b}$. The mean of $\mathbf{b}$ is vanishing. Using $\mathbf{b} = \nabla \times \mathbf{a}$, the time derivative of the volume-averaged quantity $\langle \mathbf{a} \cdot \mathbf{b} \rangle$, is found to have a term $-2\alpha \mathbf{B}_0^2$, in addition to the Spitzer term $-2\eta \langle \mathbf{j} \cdot \mathbf{b} \rangle$; see Appendix A for the derivation. Here, α refers to the α effect and it models the component of the electromotive force, $\boldsymbol{\mathcal{E}} = \langle \mathbf{u} \times \mathbf{b} \rangle$, parallel to the mean magnetic field. The α effect is responsible for the fact that the mean magnetic helicity density $\mathcal{H}_\mathrm{M} = \langle \mathbf{a} \cdot \mathbf{b} \rangle$ is no longer conserved [26].

The presence of an imposed magnetic field was found to influence the sign of the magnetic helicity and the inverse cascade [50]. For weak (or zero) imposed fields, magnetic helicity and energy cascade strongly from the forcing scale to large length scales, and the magnetic helicity has an opposite sign to the kinetic helicity. For stronger fields, the inverse cascade of magnetic helicity to larger scales is suppressed, and the sign of the mag-

netic helicity flips over. The threshold strength of the imposed magnetic field depends inversely on the square root of the magnetic Reynolds number. This is understood to be a consequence of the α effect.

It was also found that, in the presence of an imposed magnetic field, the induced magnetic field can undergo a certain enhancement around the forcing wave number. Furthermore, small-scale dynamo action helps to lower the energy density in the inertial region in k-space [50]. In addition, during the initial time interval $0 \le t \le t_*$, we drive turbulence either through the $\boldsymbol{\mathcal{F}}_0$ or $\boldsymbol{\mathcal{E}}_0$ terms.

C. Initial conditions

We consider the following types of initial conditions. First, we consider a homogeneous (imposed) magnetic field [50], where the corresponding correlation length is infinite. Second, we consider the case with no imposed field, but with a zero flux initial scale-invariant magnetic field, so the correlation length is finite, but much longer than the scale of turbulence.[4] We construct such a field in Fourier space as

$$\tilde{B}_i(\mathbf{k}) = B_\mathrm{ini} \left(\delta_{ij} - \hat{k}_i \hat{k}_j - i\sigma\epsilon_{ijl}\hat{k}_l \right) g_j(\mathbf{k}) \, |\mathbf{k}|^{-3/2}, \quad (40)$$

where $\mathbf{g}(\mathbf{k})$ is the Fourier transform of a Gaussian distributed random vector field that is δ-correlated in all three dimensions. The degree of helicity is controlled by the parameter σ, which is ± 1 for maximally helical fields with positive or negative helicity, and zero in the nonhelical case. The magnetic field in real space is given by $\mathbf{B}(\boldsymbol{x}) = \int \tilde{\mathbf{B}}(\boldsymbol{k})e^{i\boldsymbol{k}\cdot\boldsymbol{x}}d^3k/(2\pi)^3$. In all cases, we have initially $\rho = \text{const}$.

The forcing applied during $0 \le t \le t_*$ consists of monochromatic forcing (see, for example, Ref. [51]) at a wave number $k = k_\star$. This forcing wave number corresponds to a fraction of the Hubble scale $H_\star$ after inflation. One can think of this as the epoch of reheating.

In either case, we consider the relativistic fluid to have an initial turbulent velocity field $\mathbf{u}(\mathbf{x})$. Physically, turbulence can be induced at reheating by energy injection from the inflaton into the standard model particles and fields, or from bubble collisions during some (yet unknown) phase transition – the spectral energy density $E_\mathrm{M}(k)$ has a k^4 subinertial range at large scales due to causality requirements (see Refs. [52, 53]), while in the inertial range, it tends to have a Kolmogorov spectrum proportional to $k^{-5/3}$.

We recall that, in the absence of a large-scale magnetic field, a small-scale helical magnetic field undergoes inverse cascading such that the magnetic energy at small

---

[4] The finite value of the correlation length is determined by the cutoff scale imposed to the scale-invariant spectrum at the low wave numbers region [44]

TABLE I: Summary of the parameters of the simulations discussed in this paper. Some characteristic parameters, including the final values of p and q as defined below and the direction of evolution in the pq diagram are also indicated.

panel	initial field	B_0	B_{ini}	v_A^{max}	$\mathcal{F}_0$	$\mathcal{E}_0$	σ	k_*	τ_A	p	q	evolution along
(i)	homogeneous	0.1	0	0.08	0.02	0	0	60	0.19	10/7	2/7	$\beta = 4$ to $(p,q) \to (10/7, 2/7)$
(ii)	homogeneous	0.1	0	0.08	0.02	0	1	60	0.19	10/7	2/7	$\beta = 4$ to $(p,q) \to (10/7, 2/7)$
(a)	homogeneous	0.03	0	0.46	0	0.0005	1	180	0.21	2	0	$\beta = 4$ to $(p,q) \to (2/3, 2/3)$
(b)	homogeneous	0.10	0	0.41	0	0.0005	1	180	0.06	2	0	$p = 2(1-q)$ to $(p,q) \to (2,0)$
(c)	homogeneous	0.16	0	0.31	0	0.0005	1	180	0.04	4	0	$\beta = 1$–2 to $(p,q) \to (1, 0.5)$
(d)	homogeneous	0.20	0	0.25	0	0.0005	1	180	0.03	4	0	$\beta = 3$–4 to $(p,q) \to (0.1, 0.8)$
(e)	homogeneous	1.00	0	0.21	0	0.0005	1	180	0.006	4	0	$\beta = 3$–4 to $(p,q) \to (0,0)$
(A)	$1/k$ spectrum	0	10^{-3}	0.47	0	0.0005	1	180	6.4	0.6	0.6	$\beta = 0$ to $(p,q) \to (0.6, 0.6)$
(B)	$1/k$ spectrum	0	3×10^{-2}	0.37	0	0.0005	1	180	0.22	0.2	0.2	$\beta = 0$ to $(p,q) \to (0.2, 0.2)$

wave numbers increases with time [54, 55]. The characteristic length scale of the turbulence, ξ_M, increases with time like $t^{2/3}$, and the magnetic energy $\mathcal{E}_M$ decreases like $t^{-2/3}$, which is slower than in the nonhelical case where $\mathcal{E}_M \propto t^{-1}$ and $\xi_M \propto t^{1/2}$.

One often considers the magnetic field evolution in a diagram of $\mathcal{E}_M$ versus ξ_M. The nonobservation of GeV cascade photons from the interaction of TeV photons from blazars with the extragalactic background light, as mentioned above, has often been argued to imply the presence of a lower limit on the product $\mathcal{E}_M \xi_M$ of about $(10^{-15}\,\text{G})^2\,\text{Mpc}$. In a diagram of $\mathcal{E}_M$ versus ξ_M, the line corresponding to this lower limit has a slope of -1, which is also the slope of the line representing the magnetic field decay in the fully helical case, because $\mathcal{E}_M \propto t^{-2/3} \propto \xi_M^{-1}$. For a nonhelical field, on the other hand, we have $\mathcal{E}_M \propto t^{-1} \propto \xi_M^{-2}$. For this reason, a nonhelical field will eventually drop below the line demarcating the lower observational limit [45]. We now study how these decay properties are affected by the presence of either an imposed or an initial large-scale magnetic field.

D. Parameters and analysis tools

By default, we measure lengths in units of $k_1^{-1} = L/2\pi$ and wave numbers in units of k_1. Since $c = 1$, time is measured in units of the light travel time, $(ck_1)^{-1}$, and viscosity or magnetic diffusivity are measured in units of c/k_1. Furthermore, since $\rho = 1$ initially, the magnetic field is measured in units of $c/\sqrt{\rho}$. Our main control parameters are k_*, the amplitudes of the imposed or initial fields, B_0 and B_{ini}, respectively, the amplitudes of the forcing functions $\mathcal{E}_0$ and $\mathcal{F}_0$, and the values of ν and η. For k_*, we consider the values 60 and 180, B_0 and B_{ini} are varied between 0 and 1, while $\mathcal{E}_0$ and $\mathcal{F}_0$ are varied 0 and 0.02, such that the energy density of the turbulence does not exceed the radiation energy density by more than 10% after the duration of turbulent driving, which

we have chosen to be $t_* = 5$ in the normalized units defined below. In all cases, we use a resolution of 1152^3 meshpoints and we found that $\nu = \eta = 10^{-5}$ is sufficiently small to dissipate the energy of the turbulence at the smallest length scale. A summary of parameters of all runs is given in Table I.

It is sometimes convenient to express time in units of the Alfvén time, $\tau_A = (v_A k_*)^{-1}$, where $v_A^2 = B_0^2/(\frac{4}{3}\rho)$ for cases with an imposed magnetic field and $v_A^2 = B_{ini}^2/(\frac{4}{3}\rho)$ for cases with a zero flux large-scale magnetic field. To specify the strength of the fluctuating magnetic field in cases with $B_0 \neq 0$, we also specify the quantity $v_{A,f}^{max} = |\mathbf{B} - \mathbf{B}_0|/(\frac{4}{3}\rho)^{1/2}$. The kinetic and magnetic energy densities are defined as $\mathcal{E}_K = \langle \rho \mathbf{u}^2 \rangle/2$ and $\mathcal{E}_M = \langle \mathbf{B}^2 \rangle/2$, respectively, and the kinetic and magnetic energy spectra, $E_K(k,t)$ and $E_M(k,t)$, are normalized such that

$$\int E_K(k,t)\,dk = \mathcal{E}_K \quad \text{and} \quad \int E_M(k,t)\,dk = \mathcal{E}_M, \quad (41)$$

respectively. We define the magnetic correlation length ξ_M as

$$\xi_M(t) = \int k^{-1} E_M(k,t)\,dk \bigg/\!\!\bigg/ \int E_M(k,t)\,dk. \quad (42)$$

Finally, we define the instantaneous exponents describing the growth of $\xi_M(t)$ and the decay of $\mathcal{E}_M(t)$ as

$$q_i(t) = d\ln \xi_i/d\ln t, \quad p_i(t) = -d\ln \mathcal{E}_i/d\ln t. \quad (43)$$

Those play important roles in describing the nature of the turbulence in different cases [28].

The various solutions are characterized by certain lines in the pq diagram. It was found that the point (p,q) ultimately settles somewhere on what was called the self-similarity line [28], where

$$p = 2(1-q). \quad (44)$$

Moreover, this evolution occurs along a line with

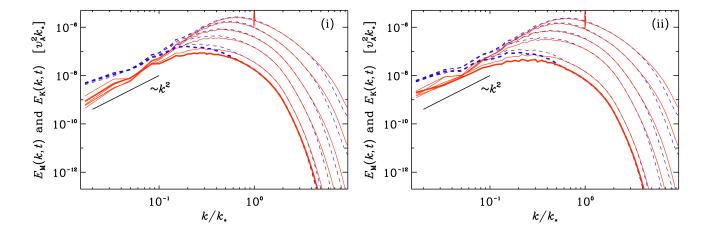$$\beta = p/q - 1 = \text{const}, \quad (45)$$

FIG. 1: The evolution of the magnetic (red) and kinetic (blue) energy spectra for (i) nonhelical and (ii) helical turbulence. The thick lines are the configurations at the latest times. Panels (i) and (ii) correspond to runs (i) and (ii) in Table I.
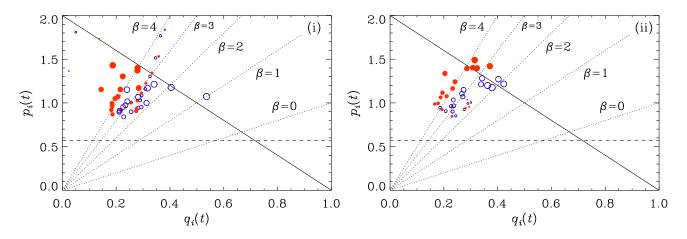

FIG. 2: pq diagrams for the cases of nonhelical (i) and helical (ii) turbulence. The dots denote the instantaneous values of (p, q) for the magnetic (red) and kinetic (blue) fields. Bigger circles denote later times. Panels (i) and (ii) correspond to runs (i) and (ii) in Table I. The solid lines correspond to the self-similarity line, $p = 2(1 - q)$, the dotted lines denote $\beta = $ const, and the dashed lines denote $p = $ const ≈ 0.58, whose relevance is explained in the text.

where the value of β is determined by the nature of certain relevant conservation laws. Eliminating p from Eqs. (44) and (45), we find $\beta = 2/q - 3$, where q can be obtained from dimensional arguments in terms of the dimensions of length L and time T. We recall that q characterizes the scaling of the correlation length with time as $\xi_{\mathrm{M}} \sim t^q$. Magnetic helicity has dimensions $L^3 T^{-2}$, so $q = 2/3$, and therefore $\beta = 0$. The mean squared vector potential, which is arguably relevant to magnetically dominated turbulence [56], has dimensions $L^4 T^{-2}$, so $q = 1/2$, and therefore $\beta = 1$. The Saffman integral [57] has dimensions $L^5 T^{-2}$, so $q = 2/5$, and therefore $\beta = 2$, while the Loitsiansky integral [58] has dimensions $L^7 T^{-2}$, so $q = 2/7$, and therefore $\beta = 4$.

Under certain conditions, the evolution may not be self-similar for extended periods of time. In fact, for finite resolution and finite domain size, a truly self-similar

behavior is generally difficult to obtain. A prolonged evolution along the line $p = $ const ≈ 0.58 was obtained [59] when there is a complex interplay between kinetic and current helicities. In the present work, we find examples of several of the aforementioned relations.

IV. RESULTS

A. Helical and nonhelical decay with imposed field

We consider decaying turbulence produced during a short initial period through forcing at small scales with $k_* = 60$ together with an imposed magnetic field. We find that in the subinertial range, the magnetic energy spectrum goes approximately as k^2, while the kinetic energy spectrum is shallower. In Figs. 1(i) and 1(ii), we

show the evolution of the magnetic and kinetic energy spectra for the nonhelical and helical cases, respectively. We see that the winding up of the initially uniform field by turbulence causes a Saffman spectrum for the magnetic energy of the form $E_M \sim k^2$, which is shallower than the Batchelor k^4 spectrum. There is no inverse cascade in the sense that, even at small k, the magnetic energy always decays. The decay is faster at larger k, which causes ξ_M to increase, but this is not due to the usual inverse cascade.

To quantify the decay further, we now show in Figs. 2(i) and 2(ii) the evolution of the instantaneous scaling exponents $p_i(t)$ versus $q_i(t)$ for $i = $ M and K, where $\mathcal{E}_i$ is the energy density and ξ_i is the integral length scale for the magnetic and fluid fields. We see that for both the helical and the nonhelical cases, the evolution of the point (p, q) tends to be close to the $\beta = 4$ line, which implies the conservation of the Loitsiansky integral [58]. This evolution is similar to that of nonhelical and nonmagnetic turbulence, which is quite surprising: in the presence of a sufficiently strong constant magnetic field, magnetic helicity seems to have no effect, and the decay is very different from that in magnetically dominated turbulence, where $\beta = 1$–2 has been found [28, 56].

B. Inverse cascade

We know that, in the absence of a large-scale magnetic field, a small-scale helical magnetic field decays more slowly than a nonhelical one, and also its correlation length increases faster than for a nonhelical field. It is therefore of interest to study how the magnetic decay is affected by the presence of this large-scale magnetic field. One may also ask whether some of the magnetic energy of this large-scale field can be transferred to the smaller scale field.

In all cases, we produce a small-scale helical magnetic field by driving the system with a turbulent small-scale electromotive force for a short time interval $0 \leq t \leq t_* = 5$. This driving is then turned off, leaving the system to decay freely, except for the presence of the imposed magnetic field. The runs are summarized in the lower part of Table I.

The time evolution of $\xi_M(t)$ and $\mathcal{E}_M(t)$ is shown in Figs. 3(a) and 3(c). In Fig. 3(b) we plot the evolution $\xi(t/\tau_A)$ versus normalized time Fig. 3(d). Our results allow us to show $\mathcal{E}_M(t)$ against $\xi_M(t)$ in a parametric fashion; see Fig. 3. Note that we have not included in $\mathcal{E}_M(t)$ the additional presence of the imposed magnetic field, i.e., the magnetic energy is defined solely based on the magnetic field with nonvanishing wave numbers.

In Figs. 4 and 5, we present magnetic energy spectra for cases with an imposed and an initial magnetic field, respectively. In both cases, we see inverse cascading of the magnetic energy when the imposed or initial magnetic fields are weak. However, when the field is increased, the inverse cascade eventually stalls; see especially Fig. 4(c),

where inverse cascading has stopped after the peak of the spectrum traversed the k axis by about a factor of 10.

Interestingly, in the presence of an initial (nonimposed) magnetic field, the evolution of $\mathcal{E}_M(t)$ versus $\xi_M(t)$ follows the same line in Fig. 3(d). This line corresponds to $\mathcal{E}_M \propto \xi_M^{-1}$ and its height in that diagram characterizes the strength of magnetic helicity [45]. Although the magnetic field was initially of small scale only, at the end of the evolution, it has reached the scale of the system. This is true for both weak and strong initial (nonhelical) magnetic fields.

For an imposed magnetic field, on the other hand, the magnetic field is always below the line $\mathcal{E}_M \propto \xi_M^{-1}$, which corresponds to the evolution of a fully helical magnetic field. This is simply because magnetic helicity is no longer conserved in that case; see the blue lines in the last panel of Fig. 3. The marked segregation between the blue and red lines in all panels of Fig. 3 is an impressive and very visual demonstration of the tremendous difference between the cases of an initial and an imposed magnetic field. Only when the imposed magnetic field is weak enough are the two cases in mutual in agreement with each other; compare the red (A) and blue (a) lines in all panels of Fig. 3.

Finally, we show in Figs. 6 and 7 the evolution of the instantaneous scaling exponents $p(t)$ and $q(t)$ in a pq diagram. We see that in the case with an imposed magnetic field of moderate strength in panel (a) the point (p, q) appears to evolve along the line $p = 2(1 - q)$ toward $(p, q) = (2, 0)$. This is indeed consistent with Fig. 3, where $\mathcal{E}_M(t)$ is seen to decay like t^{-2} and $\xi_M(t)$ is approximately flat. For a stronger imposed field in panel (b), there seems to be an evolution along $\beta = 3$–4 toward $(p, q) \rightarrow (0, 0)$, but this is not consistent with Fig. 3, where $\mathcal{E}_M(t)$ is seen to decay like t^{-4}, while $\xi_M(t)$ is still approximately flat. Indeed, the points in Fig. 6(b) have a similar size, suggesting that the evolution along the line $\beta = 3$–4 is an intermediate stage before later evolving toward $(p, q) \rightarrow (4, 0)$, which is obviously outside the plot range.

On the other hand, for an additional large-scale nonhelical magnetic field, in addition to the small-scale helical one, the evolution of the point (p, q) always occurs along the $\beta = 0$ line. As time goes on, the point (p, q) evolves further along the $\beta = 0$ line toward the left to smaller values of $p(t)$ and $q(t)$. For the weak large-scale magnetic field of panel (c), the evolution stalls near the point $(p, q) = (0.6, 0.6)$. Several intermediate points cluster along the line $p = 0.58$, which was identified in earlier work [59], but this may be coincidental. Indeed, for the stronger large-scale magnetic field of panel (d), the evolution continues toward the point $(p, q) = (0.2, 0.2)$. For sufficiently weak imposed magnetic fields, the cases of imposed and initial magnetic fields again agree with each other; compare Fig. 6(a) for run (a) with Fig. 7(A) for run (A).

These investigations have demonstrated the dramatic difference between imposed and initial large-scale mag-
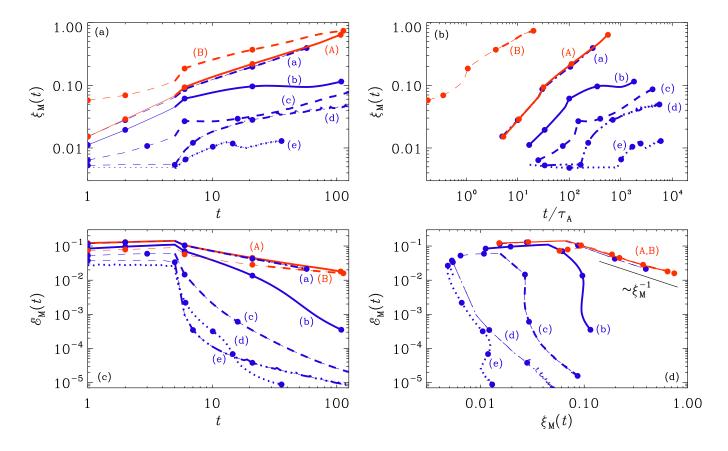
FIG. 3: Dependences of $\xi_M(t)$, $\mathcal{E}_M(t)$, $\mathcal{E}_M(t)/v_A$, and $\mathcal{E}_M(t)$ against $\xi_M(t)$. In the last panel, the slope $\mathcal{E}_M \propto \xi_M^{-2/3}$ is shown for comparison. The time interval $0 \leq t \leq t_* \equiv 5$ is marked with thin lines, while later times are marked with thick lines. Blue (red) lines denote cases with a perfectly homogeneous (statistically homogeneous) magnetic field. Solid (dashed) lines correspond to cases with a weak (strong) magnetic field; compare labels (a)–(d) with the corresponding runs in Table I. The filled symbols on each curve denote the five instances for which the spectra below are shown.

netic fields. When the imposed fields are weak, it only affects the evolution of the small-scale helical magnetic field at later times once its field strength approaches the value of the imposed field. In the presence of a large-scale nonhelical magnetic field – here one with a k^{-1} spectrum – the inverse cascade is not suppressed. Both for weak and strong magnetic fields, there is a spectral peak moving from large to small wave numbers; see Fig. 5. Also the evolution in the pq diagram is along the $\beta = 0$ line in both cases; see Fig. 7.

We emphasize again that the presence of an imposed field is pathological, if the interest is to simulate an approximation to the case with a large-scale magnetic field. We have demonstrated this here with an irregular large-scale field with a k^{-1} spectrum. Starting with an initially sinusoidal magnetic field is probably similar in many ways, but this would introduce anisotropies, which have not yet been studied in the context of decaying turbulence.

V.   CONCLUSIONS

We have discussed the viability of a homogeneous magnetic field after inflation. Our work therefore extends the earlier work of one of the authors [32], which addressed only the stability of the magnetic field in the inflationary stage. In this work, we have addressed the phenomenology of the primordial plasma after inflation in the presence of a homogeneous magnetic field. Our results apply to the early epochs of the Universe all the way from the time when the inequality in Eq. (32) is satisfied until matter radiation equality.

Our simulations have verified that, in the presence of an imposed magnetic field, magnetic helicity is not conserved. Moreover, and this was not previously known, our results demonstrate that the decay of magnetic energy in the fluctuations is faster the stronger the imposed magnetic field. We have also compared the magnetic field evolution with an alternative way of simulating a cosmological large-scale magnetic field, namely to treat it as a statistically homogeneous field with a scale-invariant spectrum. It is no longer the stealth magnetic field con-
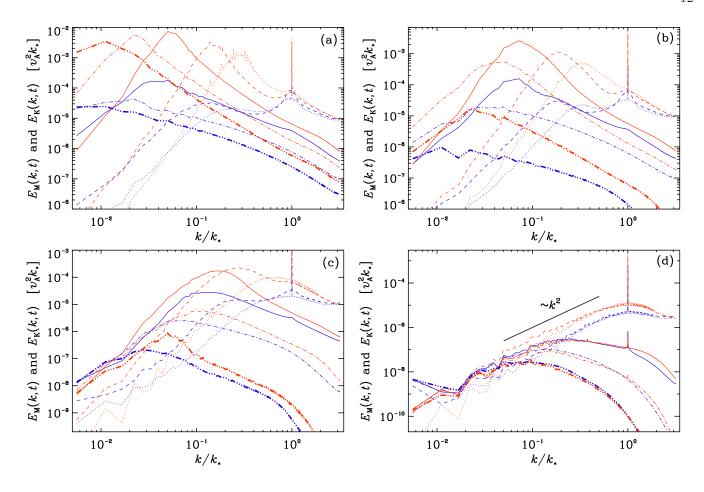
FIG. 4: Magnetic (red) and kinetic (blue) energy spectra for $k_*/k_1 = 180$ with an imposed field, $B_0 = 0.03$, 0.1, 0.16, and 0.2 in panels (a)–(d), respectively. These panels correspond to runs (a)–(d) in Table I. Dotted, dashed, solid, dash-dotted, and dash-triple-dotted lines indicate later times, denoted by filled symbols in Fig. 3. The last time is also shown as a fat line.
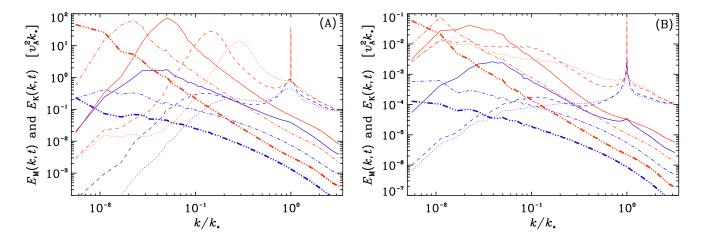

FIG. 5: Similar to Fig. 4, but for an initial large-scale field, $B_{ini} = 10^{-3}$ and 3×10^{-2} in panels (A) and (B), respectively.

sidered in the scenario of [22], but one that could emerge at the end of inflation. Such a magnetic field can be either helical [44, 53] or nonhelical [25]. In these cases, magnetic helicity conservation is unaffected by the large-scale magnetic field, and it decays just like without imposed magnetic field and thus much more slowly than with a constant imposed magnetic field.

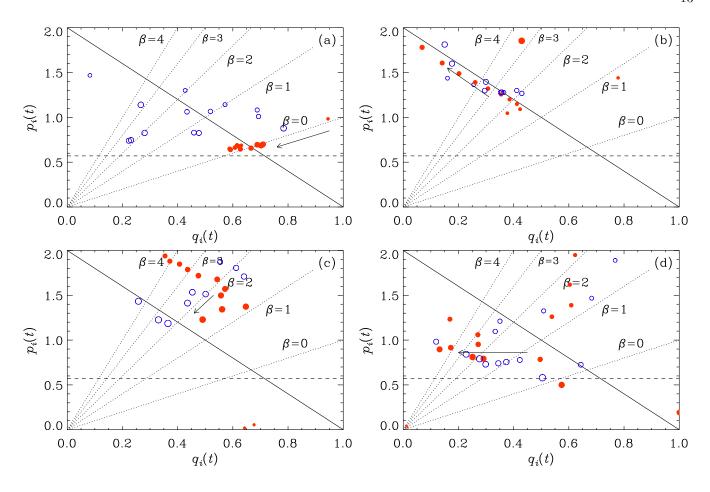Conservation of magnetic helicity (and correspond-

FIG. 6: *pq* diagrams for the magnetic field (red) and the velocity field (blue) for $k_*/k_1 = 180$ with an imposed field, $B_0 = 0.03$, 0.1, 0.16, and 0.2 in panels (a)–(d), respectively. Again, these panels correspond to runs (a)–(d) in Table I. Later times are shown as larger symbols. The arrows in each panel indicate the tentative direction of evolution.
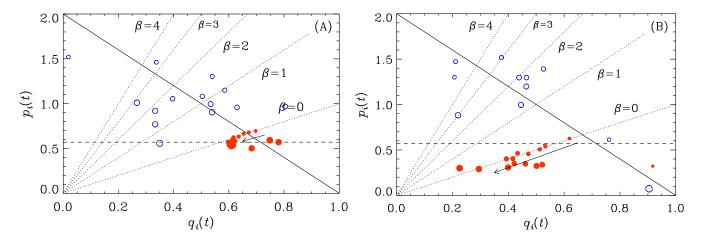

FIG. 7: Similar to Fig. 6, but for an initial large-scale field, $B_{\rm ini} = 10^{-3}$ and 3×10^{-2} in panels (A) and (B),

ingly its presence until recombination) can have important observational consequences. In particular, primordial magnetic helicity (as a manifestation of the possible violation of parity in the early Universe) can leave traces

in (i) the cosmic microwave background fluctuations, resulting in nonzero temperature B-polarization, and E- and B-polarization cross correlations (see [60, 61] and references therein), and (ii) the circular polarization of grav-

itational waves generated in the early Universe through helical hydrodynamical and MHD turbulence (see [62] and references therein).

As for the backreaction of small-scale fields to the background magnetic field at large scale, *a priori* there could be three possibilities: (i) small-scale fields inverse cascade and deplete the background magnetic field at large scale; (ii) small-scale fields inverse cascade and enhance the background magnetic field at large scale; or (iii) small-scale fields do not affect the background magnetic field at large scale. The result of the present paper suggests that (iii) is the case. Therefore, a homogeneous magnetic field, if generated during inflation, should persist [i.e., simply decay as $\propto 1/a^2$, as assumed in the derivation of (23)] under the influence of small-scale fields and could be the origin of the large-scale magnetic field in the Universe today. Depending on the strength of the background magnetic field, however, the small-scale magnetic field can be significantly suppressed. The low power at small scales (see the blue lines in Fig. 3) means that the homogeneous background may dominate the magnetic fields in the Universe not only at large scales but also at small scales. This implies that, depending on its strength, the background magnetic field may be responsible not only for the blazar observations, but also for the seeds of MHD processes at astrophysical scales such as galactic dynamo.

Appendix A: Magnetic helicity evolution in the presence of a homogeneous magnetic field

The purpose of this appendix is to recall why magnetic helicity is not a conserved quantity in the presence of a homogeneous or imposed magnetic field, $\mathbf{B}_0$. We write $\mathbf{B} = \mathbf{B}_0 + \mathbf{b}$, where $\mathbf{b} = \boldsymbol{\nabla} \times \mathbf{a}$, with $\mathbf{a}$ being the vector potential of $\mathbf{b}$. Equation (36) can then be written in terms of $\mathbf{a}$ as

$$\frac{\partial \mathbf{a}}{\partial t} = \mathbf{u} \times \mathbf{B}_0 + \mathbf{u} \times \mathbf{b} - \eta \mathbf{j} + \boldsymbol{\mathcal{E}}_0. \qquad \text{(A1)}$$

We consider times $t > t_*$ when $\boldsymbol{\mathcal{E}}_0 = \mathbf{0}$. Making use of the periodic boundary conditions for $\mathbf{a}$, the evolution equation for $\langle \mathbf{a} \cdot \mathbf{b} \rangle$ is then

$$\frac{d}{dt}\langle \mathbf{a} \cdot \mathbf{b} \rangle = 2\langle (\mathbf{u} \times \mathbf{B}_0) \cdot \mathbf{b} \rangle - 2\eta \langle \mathbf{j} \cdot \mathbf{b} \rangle. \qquad \text{(A2)}$$

Evidently, the first term on the right-hand side of Eq. (A2) breaks magnetic helicity conservation in the limit $\eta \to 0$, because

$$\langle (\mathbf{u} \times \mathbf{B}_0) \cdot \mathbf{b} \rangle = -\langle \mathbf{u} \times \mathbf{b} \rangle \cdot \mathbf{B}_0 = -\alpha \mathbf{B}_0^2 \neq 0 \qquad \text{(A3)}$$

for a helical magnetic field, where $\alpha \neq 0$. We recall an important result from mean-field electrodynamics [63, 64]

$$\langle \mathbf{u} \times \mathbf{b} \rangle_i = \alpha_{ij} \langle B_j \rangle + \beta_{ijk} \partial \langle B_j \rangle / \partial x_k + \cdots, \qquad \text{(A4)}$$

which reduces to $\langle \mathbf{u} \times \mathbf{b} \rangle = \alpha \mathbf{B}_0$ for periodic boundary conditions. Here, the ellipsis refers to higher order terms. The nonconservation of magnetic helicity is not an artifact of having adopted periodic boundary conditions, because they are just a tool for us to compute averages over infinitely large length scales.

[1] L. M. Widrow, "Origin of galactic and extragalactic magnetic fields," Rev. Mod. Phys. **74**, 775 (2002).

[2] R. Durrer and A. Neronov, "Cosmological Magnetic Fields: Their Generation, Evolution and Observation," Astron. Astrophys. Rev. **21**, 62 (2013).

[3] R. M. Kulsrud and E. G. Zweibel, "The Origin of Astrophysical Magnetic Fields," Rept. Prog. Phys. **71**, 046091 (2008).

[4] A. Kandus, K. E. Kunze and C. G. Tsagas, "Primordial magnetogenesis," Phys. Rept. **505**, 1 (2011).

[5] A. Neronov and I. Vovk, "Evidence for strong extragalactic magnetic fields from Fermi observations of TeV blazars," Science **328**, 73 (2010).

[6] C. D. Dermer, M. Cavadini, S. Razzaque, J. D. Finke, J. Chiang and B. Lott, "Time Delay of Cascade Radiation for TeV Blazars and the Measurement of the Intergalactic Magnetic Field," Astrophys. J. **733**, L21 (2011).

[7] A. M. Taylor, I. Vovk and A. Neronov, "Extragalactic magnetic fields constraints from simultaneous GeV-TeV observations of blazars," Astron. Astrophys. **529**, A144 (2011).

[8] S. Archambault *et al.* [VERITAS Collaboration], "Search for Magnetically Broadened Cascade Emission From Blazars with VERITAS," Astrophys. J. **835**, 288 (2017).

[9] M. Ackermann *et al.* [Fermi-LAT Collaboration], "The Search for Spatial Extension in High-latitude Sources Detected by the *Fermi* Large Area Telescope," Astrophys. J. Suppl. **237**, 32 (2018).

[10] K. Dolag, M. Kachelriess, S. Ostapchenko and R. Tomas, "Lower limit on the strength and filling factor of extragalactic magnetic fields," Astrophys. J. **727**, L4 (2011).

[11] T. C. Arlen, V. V. Vassiliev, T. Weisgarber, S. P. Wakely and S. Y. Shafi, "Intergalactic Magnetic Fields and Gamma Ray Observations of Extreme TeV Blazars," Astrophys. J. **796**, 18 (2014).

[12] A. E. Broderick, P. Tiede, P. Chang, A. Lamberts, C. Pfrommer, E. Puchwein, M. Shalaby and M. Werhahn, "Missing Gamma-ray Halos and the Need for New Physics in the Gamma-ray Sky," Astrophys. J. **868**, 87 (2018).

[13] R. Alves Batista, A. Saveliev and E. M. de Gouveia Dal Pino, "The Impact of Plasma Instabilities on the Spectra of TeV Blazars," Mon. Not. Roy. Astron. Soc. **489**, 3836 (2019).

[14] K. Subramanian, "The origin, evolution and signatures of primordial magnetic fields," Rept. Prog. Phys. **79**, 076901 (2016).

[15] T. Kahniashvili, A. Brandenburg, A. Kosowsky, S. Mandal and A. R. Pol, "Magnetism in the Early Universe," in Astronomy in Focus, Vol. 14, Proc. IAU Symp. (Cambridge University Press, 2020), ed.: M.T. Lago, 295–298 (2020).

[16] Zel'dovich Ya.B., "Magnetic Model of the Universe," Sov. Phys. JETP **48**, 986 (1965).

[17] Doroshkevich A., "Model of a Universe with a uniform magnetic field," Astrophysics **1**, 138 (1965).

[18] K. S. Thorne, "Primordial Element Formation, Primordial Magnetic Fields, and the Isotropy of the Universe," Astrophys. J. **148**, 51 (1967).

[19] Harrison, E. R., "Generation of magnetic fields in the radiation ERA," Mon. Not. Roy. Astron. Soc. **147**, 279 (1970).

[20] O. Bertolami and D. F. Mota, "Primordial magnetic fields via spontaneous breaking of Lorentz invariance," Phys. Lett. B **455**, 96 (1999).

[21] K. i. Maeda and K. Yamamoto, "Inflationary Dynamics with a Non-Abelian Gauge Field," Phys. Rev. D **87**, 023528 (2013).

[22] S. Mukohyama, "Stealth magnetic field in de Sitter spacetime," Phys. Rev. D **94**, 121302 (2016).

[23] Y. Fujii and K. Maeda, "The scalar-tensor theory of gravitation," Cambridge University Press (2003).

[24] C. Armendariz-Picon, V. F. Mukhanov and P. J. Steinhardt, "Essentials of k essence," Phys. Rev. D **63**, 103510 (2001).

[25] T. Kahniashvili, A. Brandenburg, L. Campanelli, B. Ratra and A. G. Tevzadze, "Evolution of inflation-generated magnetic field through phase transitions," Phys. Rev. D **86**, 103005 (2012).

[26] M. A. Berger, "Magnetic helicity in a periodic domain" J. Geophys. Res. A **102** 2637, (1997).

[27] D. Biskamp and W.-C. Müller, "Decay laws for three-dimensional magnetohydrodynamic turbulence", Phys. Rev. Lett. **83**, 2195 (1999).

[28] A. Brandenburg and T. Kahniashvili, "Classes of hydrodynamic and magnetohydrodynamic turbulent decay," Phys. Rev. Lett. **118**, 055102 (2017).

[29] G. W. Horndeski, "Second-order scalar-tensor field equa-tions in a four-dimensional space," Int. J. Theor. Phys. **10**, 363 (1974).

[30] C. Deffayet, X. Gao, D. A. Steer and G. Zahariade, "From k-essence to generalised Galileons," Phys. Rev. D **84**, 064039 (2011).

[31] G. W. Horndeski, "Conservation of Charge and the Einstein-Maxwell Field Equations," J. Math. Phys. **17**, 1980 (1976).

[32] S. Mukohyama, "Stability of stealth magnetic field in de Sitter spacetime," Phys. Rev. D **98**, 104053 (2018).

[33] J. R. Shaw and A. Lewis, "Constraining Primordial Magnetism," Phys. Rev. D **86**, 043510 (2012).

[34] J. Adamek, R. Durrer, E. Fenu and M. Vonlanthen, "A large scale coherent magnetic field: interactions with free streaming particles and limits from the CMB," JCAP **1106**, 017 (2011).

[35] N. Aghanim *et al.* [Planck Collaboration], "Planck 2018 results. VI. Cosmological parameters," arXiv:1807.06209 [astro-ph.CO] (2020).

[36] F. Tavecchio, G. Ghisellini, L. Foschini, G. Bonnoli, G. Ghirlanda and P. Coppi, "The intergalactic magnetic field constrained by Fermi/LAT observations of the TeV blazar 1ES 0229+200," Mon. Not. Roy. Astron. Soc. **406**, L70 (2010).

[37] S. Ando and A. Kusenko, "Evidence for Gamma-Ray Halos Around Active Galactic Nuclei and the First Measurement of Intergalactic Magnetic Fields," Astrophys. J. **722**, L39 (2010).

[38] W. Essey, S. Ando and A. Kusenko, "Determination of intergalactic magnetic fields from gamma ray data," Astropart. Phys. **35**, 135 (2011).

[39] K. Takahashi, M. Mori, K. Ichiki, S. Inoue and H. Takami, "Lower Bounds on Magnetic Fields in Intergalactic Voids from Long-term GeV-TeV Light Curves of the Blazar Mrk 421," Astrophys. J. **771**, L42 (2013).

[40] W. Chen, J. H. Buckley and F. Ferrer, "Search for GeV γ-Ray Pair Halos Around Low Redshift Blazars," Phys. Rev. Lett. **115**, 211103 (2015).

[41] J. D. Barrow, M. Thorsrud and K. Yamamoto, "Cosmologies in Horndeski's second-order vector-tensor theory," JHEP **1302**, 146 (2013).

[42] A. Allahyari, M. A. Gorji and S. Mukohyama, "Bounds on the Horndeski Gauge-Gravity Coupling," JCAP **05**, 013 (2020).

[43] A. Brandenburg, K. Enqvist and P. Olesen, "Large scale magnetic fields from hydromagnetic turbulence in the very early universe," Phys. Rev. D **54**, 1291 (1996).

[44] T. Kahniashvili, A. Brandenburg, R. Durrer, A. G. Tevzadze and W. Yin, "Scale-invariant helical magnetic field evolution and the duration of inflation," JCAP **1712**, 002 (2017).

[45] A. Brandenburg, T. Kahniashvili, S. Mandal, A. R. Pol, A. G. Tevzadze and T. Vachaspati, "Evolution of hydromagnetic turbulence from the electroweak phase transition," Phys. Rev. D **96**, 123528 (2017).

[46] A. Brandenburg, "The Inverse cascade and nonlinear alpha-effect in simulations of isotropic helical hydromagnetic turbulence," Astrophys. J. **550**, 824 (2001).

[47] D. Moss, "A numerical model of hydromagnetic turbulence", Mon. Not. Roy. Astron. Soc. **148**, 173 (1970).

[48] M. W. Matthaeus and M. L. Goldstein, "Measurement of the rugged invariants of magnetohydrodynamics in the solar wind," J. Geophys. Res. B **87**, 6011 (1982).

[49] A. Brandenburg and W. H. Matthaeus, "Magnetic helic-

ity evolution in a periodic domain with imposed field," Phys. Rev. E **69**, 056407 (2004).

[50] N. E. L. Haugen and A. Brandenburg, "Suppression of small scale dynamo action by an imposed magnetic field," Phys. Rev. E **70**, 036408 (2004).

[51] T. Kahniashvili, A. Brandenburg, A. G. Tevzadze and B. Ratra, "Numerical simulations of the decay of primordial magnetic turbulence," Phys. Rev. D **81**, 123002 (2010).

[52] R. Durrer and C. Caprini, "Primordial magnetic fields and causality," JCAP **0311**, 010 (2003).

[53] A. Brandenburg, R. Durrer, T. Kahniashvili, S. Mandal and W. W. Yin, "Statistical Properties of Scale-Invariant Helical Magnetic Fields and Applications to Cosmology," JCAP **1808**, 034 (2018).

[54] M. Christensson, M. Hindmarsh and A. Brandenburg, "Inverse cascade in decaying 3-D magnetohydrodynamic turbulence," Phys. Rev. E **64**, 056405 (2001).

[55] R. Banerjee and K. Jedamzik, "The Evolution of cosmic magnetic fields: From the very early universe, to recombination, to the present," Phys. Rev. D **70**, 123003 (2004).

[56] A. Brandenburg, T. Kahniashvili and A. G. Tevzadze, "Nonhelical inverse transfer of a decaying turbulent magnetic field," Phys. Rev. Lett. **114**, 075001 (2015).

[57] P. G. Saffman, "Note on decay of homogeneous turbulence," Phys. Fluids **10**, 1349 (1967).

[58] G. K. Batchelor and I. Proudman, "The large-scale structure of homogeneous turbulence," Phil. Trans. R. Soc. A **248**, 369 (1956).

[59] A. Brandenburg, T. Kahniashvili, S. Mandal, A. Roper Pol, A. G. Tevzadze and T. Vachaspati, "The dynamo effect in decaying helical turbulence," Phys. Rev. Fluids. **4**, 024608 (2019).

[60] T. Kahniashvili, Y. Maravin, G. Lavrelashvili and A. Kosowsky, "Primordial Magnetic Helicity Constraints from WMAP Nine-Year Data," Phys. Rev. D **90**, 083004 (2014).

[61] M. Ballardini, F. Finelli and D. Paoletti, "CMB anisotropies generated by a stochastic background of primordial magnetic fields with non-zero helicity," JCAP **10**, 031 (2015).

[62] A. Roper Pol, S. Mandal, A. Brandenburg, T. Kahniashvili and A. Kosowsky, "Numerical Simulations of Gravitational Waves from Early-Universe Turbulence," [arXiv:1903.08585 [astro-ph.CO]].

[63] H. K. Moffatt, *Magnetic Field Generation in Electrically Conducting Fluids*. Cambridge: Cambridge Univ. Press (1978).

[64] F. Krause and K.-H. Rädler, *Mean-field Magnetohydrodynamics and Dynamo Theory*. Oxford: Pergamon Press (1980).